行政院國家科學委員會專題研究計畫 成果報告

使用反質子交換週期性區域反轉鈮酸鋰波導及修正場自相關技術突破飛秒脈衝量測靈敏度極限
研究成果報告(精簡版)

計 畫 類 別 ：個別型
計 畫 編 號 ：NSC 98-2221-E-007-031-
執 行 期 間 ：98 年 08 月 01 日至 99 年 07 月 31 日
執 行 單 位 ：國立清華大學光電研究所

計 畫 主 持 人：楊尚達

計畫參與人員：博士班研究生-兼任助理人員：許呈韶

處 理 方 式 ：本計畫涉及專利或其他智慧財產權，1 年後可公開查詢

中 華 民 國 99 年 11 月 08 日

附件一

行政院國家科學委員會補助專題研究計畫☑ 成 果 報 告 □期中進度報告

使用反質子交換週期性區域反轉鈮酸鋰波導及修正場自相關技術突破飛秒脈衝量測靈敏度極限

計畫類別：☑個別型計畫　□整合型計畫
計畫編號：NSC 98－2221－E－007－031
執行期間：98 年 08 月 01 日至 99 年 07 月 31 日

執行機構及系所：

計畫主持人：楊尚達
共同主持人：Martin. M. Fejer、Carsten Langrock
計畫參與人員：許呈韶、林仕倫

成果報告類型(依經費核定清單規定繳交)：□精簡報告　☑完整報告

本計畫除繳交成果報告外，另須繳交以下出國心得報告：
□赴國外出差或研習心得報告
□赴大陸地區出差或研習心得報告
□出席國際學術會議心得報告
□國際合作研究計畫國外研究報告

處理方式：除列管計畫及下列情形者外，得立即公開查詢
☑涉及專利或其他智慧財產權，☑一年□二年後可公開查詢

中　華　民　國　99 年　10 月　30 日

■ 中文摘要：

關鍵字：超快光學、非線性光學、光脈衝量測、准相位匹配

本計畫的主要目標為結合本實驗室建立之「修正干涉場自相關」 (modified interferometric field autocorrelation)技術，及史丹福大學 Prof. Martin M. Fejer 實驗室獨具之「反質子交換週期性區域反轉鈮酸鋰波導」技術，以突破現有之（無參考光）飛秒脈衝完全量測技術靈敏度的世界紀錄數十倍。此一預期之靈敏度突破並非依賴昂貴之量測模組(如 intensified CCD)或冗長的量測積分時間，而是訴諸「修正干涉場自相關」技術在理論上的創新（達到使用二階非線性光學特性量測脈衝之極限）及「反質子交換週期性區域反轉鈮酸鋰波導」無匹的倍頻轉換效率(6400 %/W)。光脈衝量測上的進展尚有助於量測非週期性准相位匹配光柵的複數相位匹配頻譜，提供研究鐵電材料區域一個強大的檢測工具。考量到史丹福團隊製作波導晶片(目前並無商用產品或其他研究單位可提供)及本實驗室降低光電倍增管雜訊所需，這些研究目標難以由現行計畫贊助實現。

■ 英文摘要：

Keywords: ultrafast optics, nonlinear optics, pulse measurement, quasi-phase matching

The ambitious goal of this proposal is to improve on the world record of sensitivity of self-referenced complete femtosecond pulse measurement techniques by tens of times via the marriage of modified interferometric field autocorrelation (MIFA) method and the proprietary reverse proton exchange (RPE) periodically poled lithium niobate (PPLN) waveguide technology that have been established by our group at National Tsing Hua University and Prof. Martin M. Fejer's group at Stanford University, respectively. The sensitivity improvement will not rely on expensive detection module nor impractically long integration time, but theoretical novelty of MIFA method that hits the sensitivity limit of pulse measurement using second-order nonlinearity as well as the unparalleled conversion efficiency of RPE PPLN waveguide. The pulse measurement work will also enable full characterization of complex phase-matching spectrum of arbitrary quasi-phase matching (QPM) grating, providing a powerful tool for ferroelectric domain engineering. These research goals, however, can hardly be accomplished by the funding of our existing NSC project considering the costs of our Stanford collaborators to make RPE PPLN waveguides (no commercial product, nor can be provided by other research group) and the thermal noise reduction module for our photomultiplier tube.

報告內容：

一、前言

This report summarizes the theoretical and experimental results of the project entitled “Record sensitive femtosecond pulse measurement by reverse proton exchanged periodically poled lithium niobate waveguide and modified interferometric field autocorrelation method”, sponsored by National Science Committee under grant NSC 98-2221-E-007-031.

二、研究目的

Determination of the complex field of ultrashort optical pulse is essential in a variety of applications, such as coherently controlled nonlinear spectroscopy [1], and adaptive pulse compression [2]. Since the time duration of ultrafast signal is much shorter than the response time of existing photodetectors (~10 ps), nonlinear optical techniques are usually employed to perform “temporal gating” or “spectral shearing” to retrieve the pulse information. As a result, most of the existing measurement schemes are subject to poor sensitivity limited by the low nonlinear conversion efficiency of thin nonlinear crystals required to phase-match the broad spectra of femtosecond pulses. **Our work is aimed to break the world record of sensitivity of self-referenced complete femtosecond pulse measurement techniques** by the marriage of our MIFA method [3] and the proprietary reverse proton exchange (RPE) PPLN waveguide technology [4] of Prof. Martin M. Fejer’s group at Stanford University. We expect to improve on the current world record [5, 6] **by tens of times**.

三、文獻探討

I. Intensity autcorrelation (IA):

Fig. 1 illustrates the collinear intensity autocorrelator. The Michelson interferometer (MI) splits and recombines the input pulse of field envelope $a(t)$ to produce a pulse pair:

$$a_{\omega}(t,\tau) = a(t) + a(t-\tau)e^{-j\omega_0\tau},$$

where ω_0 is the carrier angular frequency. A thin second-harmonic generation (SHG) crystal with sufficiently broad phase-matching(PM) bandwidth can produce a second-harmonic pulse with field envelope:

$$a_{2\omega}(t,\tau) \propto a_{\omega}^2(t,\tau).$$

Measuring the second-harmonic average power by a slow point detector gives rise to a fringe-resolved intensity autocorrelation trace:

$$\langle P_{2\omega}(\tau)\rangle_{FR} \propto \int_{-\infty}^{\infty} \left|a_{\omega}^2(t,\tau)\right|^2 dt.$$

By low-pass filtering the raw trace $\langle P_{2\omega}(\tau)\rangle_{FR}$, we can derive a fringe-free trace of the form:

$$\langle P_{2\omega}(\tau)\rangle \propto 1+2G_2(\tau),$$

where

$$G_2(\tau) \equiv \langle I(t)I(t-\tau)\rangle \big/ \langle I^2(t)\rangle \tag{1}$$

is the normalized intensity autocorrelation function [$I(t)=|a(t)|^2$]. For well-behaved pulse shapes, the pulse width Δt can be roughly estimated (with an uncertainty of ~10%) by deconvolution of the correlation width $\Delta\tau$ of $G_2(\tau)$. Nevertheless, $G_2(\tau)$ only delivers very limited pulse information for lack of information about temporal phase of $a(t)$ and spectral phase of intensity $I(t)$.

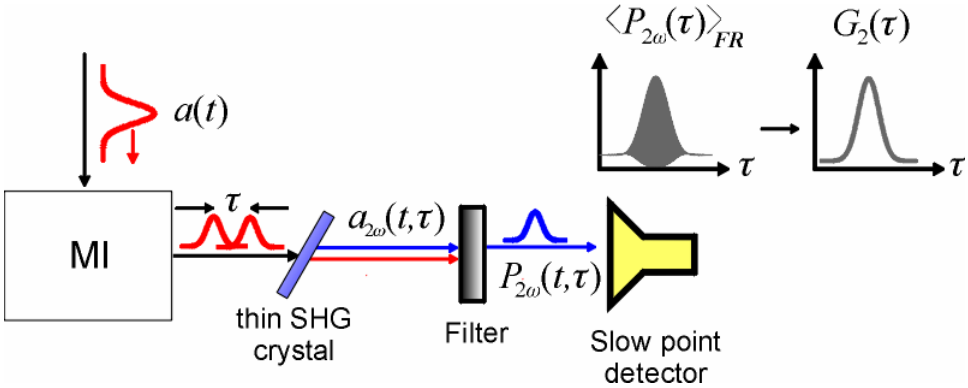

Fig. 1. Schematic diagram of intensity autocorrelation measurement. MI: Michelson interferometer.

Intensity autocorrelation measurement is intrinsically more sensitive than other techniques designed to deliver "complete" pulse information, for it does not need frequency-resolved optics and only relies on slow point detector, which can be made extremely sensitive when using photomultiplier tube and lock-in amplifier. As a result, intensity autocorrelation measurement using thin bulk SHG crystals offers a sensitivity of about 1 mW^2. Significant improvement of sensitivity has been achieved by using SHG in A-PPLN waveguide (3.2×10^{-7} mW^2) [7], where 50-MHz, 220-fs pulse train at 1.5-μm can be measured with an average power as low as 1.3 nW (equivalent to 0.24-mW peak power, 52 aJ or 400 photons per pulse).

II. Frequency resolved optical gating (FROG):

FROG [8] is a time-frequency technique to derive complete amplitude and phase information. It applies the strategy of: (1) using the unknown pulse itself for ultrafast gating; (2) recording data points more than the degrees of freedom (data redundancy), then retrieving the complex field by iteration. Fig. 2 shows the schematic diagram of conventional second-harmonic generation (SHG) FROG. The noncollinear SHG geometry can spatially separate the field product term $a(t)\cdot a(t-\tau)$ from the remaining self-squared terms $a^2(t)$, $a^2(t-\tau)$. By measuring the second-harmonic power spectrum for each delay τ, we obtain the FROG trace:

$$I_{FROG}(\omega,\tau) = \left|F\{a(t)\cdot a(t-\tau)\}\right|^2 \tag{2}$$

where $F\{\ldots\}$ denotes Fourier transform with respect to variable t. Finally, some iterative algorithm is used to retrieve the exact complex field $a(t)$.

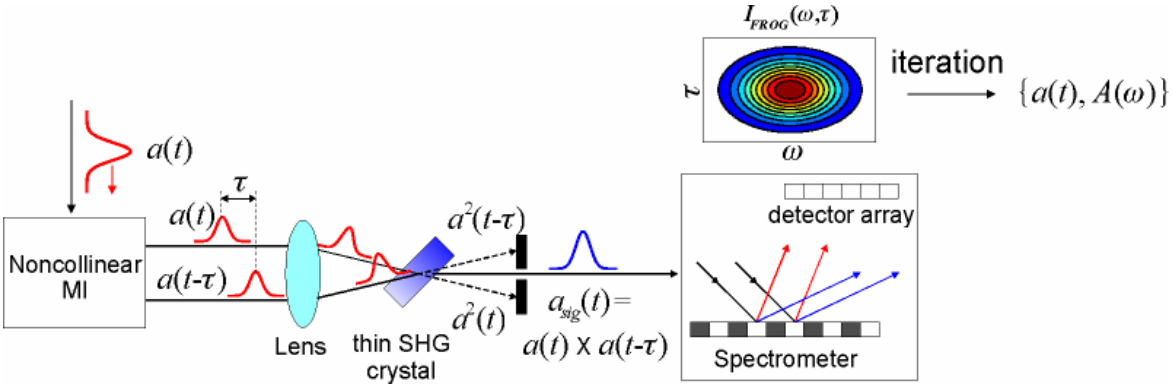

Fig. 2. Schematic diagram of conventional SHG FROG.

FROG is extremely robust against system error and measurement noise because of the built-in data redundancy, which provides consistency check and excludes the impossible solution corresponding to the noise-contaminated trace [8].

In principle, FROG is less sensitive than intensity autocorrelation due to the requirement of acquiring power spectra (compared with average powers in IA). However, SHG FROG using long aperiodically-poled lithium niobate (A-PPLN) waveguides [5,6,9] can significantly improve the sensitivity. A-PPLN waveguides consist of: (a) QPM grating with chirped poling period such that long crystal can still have broad phase-matching bandwidth. (b) Single-mode waveguide made by proton exchange process, allowing for nonlinear interaction between fundamental and second-harmonic beams within a small cross-sectional area over a long interaction distance. Pulse train of 50-MHz repetition rate, 280-fs duration at 1.5-μm wavelength with an average power of 6.2 nW (equivalent to 0.44-mW peak power, 124 aJ or 960 photons per pulse) has been fully characterized, corresponding to a sensitivity of 2.7×10^{-6} mW^2) without any reference pulse [9].

III. Spectral phase interferometry for direct electric-field reconstruction (SPIDER):

SPIDER [10] is an interferometric technique to retrieve spectral phase by algebraic (non-iterative) data inversion. Fig. 3 illustrates its schematic diagram. The input pulse is split into two replicas with fixed delay τ, and mixed with a highly chirped pulse (usually obtained by passing another input pulse replica through a dispersive medium) to perform frequency conversion (typically sum- or difference- frequency generation). Since the chirped pulse has different local frequencies at different time instants, the two output pulse replicas are spectrally separated by a frequency shearing Ω, leading to an interferogram:

$$S(\omega)=\left|A(\omega)\right|^2+\left|A(\omega+\Omega)\right|^2+2\left|A(\omega)A(\omega+\Omega)\right|\cos\left[\psi(\omega+\Omega)-\psi(\omega)+\omega\tau\right], \qquad (3)$$

where $A(\omega)$ and $\psi(\omega)$ are the complex spectrum and spectral phase of the input pulse at baseband (carrier-frequency removed), respectively. Eq. (3) can be processed by Fourier transform and filtering to get the differential spectral phase function:

$$\Delta\psi(\omega)=\psi(\omega)-\psi(\omega-\Omega),$$

from which the exact spectral phase $\psi(\omega)$ (with a resolution of Ω) can be derived by

concatenation.

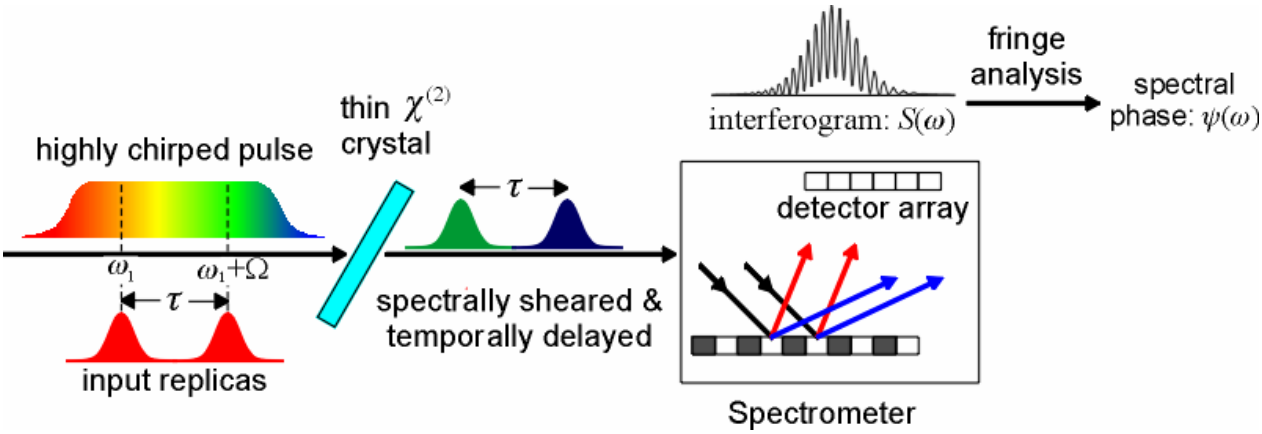

Fig. 3. Schematic diagram of SPIDER.

Only a limited number of approaches, such as homodyne optical technique (HOT) SPIDER [11], electro-optic shearing interferometry [12], have been proposed to improve the sensitivity of SPIDER. However, they rely on either a strong reference pulse [11], or a high-speed phase modulator [12], which is not self-referenced or subject to poor temporal resolution (400 fs). SPIDER using thick nonlinear crystal has been reported [13], but its merit largely lies on elimination of the highly chirped pulse in spectral shearing (instead of sensitivity improvement) and is only applicable for particular combination of the crystal's material, length, and the wavelength range. **In standard SPIDER, either type-2 or noncollinear type-1 phase matching has to be utilized** for nonlinear mixing, such that the undesired SHG signal due to self-interaction can be either suppressed (not phase-matched) or spatially separated from the desired sum-frequency generation signal given they are spectrally degenerated. Since straight lithium niobate waveguide made by proton exchange only guides TM polarization (only n_e is increased), type-2 phase matching is prohibited. Furthermore, typical straight waveguides only supports collinear geometry (unless using asymmetric Y-junction devices [14,15]), disabling the employment of collinear type-1 phase matching as well. As a result, **SPIDER cannot employ the highly efficient RPE PPLN straight waveguide** [4].

IV. High-efficiency wavelength conversion by reverse proton exchange (RPE) PPLN waveguide: (This section is based on materials provided by M. M. Fejer's group.)

Second-order nonlinear waveguide devices are the key components for the ultrashort pulse measurement scheme suggested in this proposal. Prof. Fejer's group at Stanford University has developed a number of techniques to enable efficient nonlinear optical mixing processes, and in particular to optimize devices operating in the 1.5-μm communications band. The two key steps are microstructuring the nonlinear medium to enable quasi-phase matching (QPM) and fabrication of waveguides to confine the light over long interaction lengths to increase the nonlinear mixing efficiency. We briefly review these techniques, which will be the keys to achieve record sensitivity of femtosecond pulse measurement.

Quasi-phase-matching (QPM)

In second order nonlinear optics, e.g., second-harmonic generation (SHG), material dispersion causes the phase between the nonlinear polarization and the electric field at the newly generated frequency to drift with propagation distance, preventing continuous growth of the newly generated field. The distance over which the accumulated phase difference between the second harmonic and the driving polarization changes by π is called the coherence length l_c. In QPM, continuous growth of the generated field along the propagation direction is achieved by resetting the phase of the driving polarization every coherence length via changing the sign of the nonlinear coefficient. In the wave-vector space, QPM is equivalent to compensating the wave-vector mismatch Δk between the nonlinear polarization [$2k_\omega = 2\omega n(\omega)/c$] and the second-harmonic field wave [$k_{2\omega} = 2\omega n(2\omega)/c$] by applying an artificial wave-vector K_g arising from a grating with appropriate period $\Lambda_g = 2l_c$ (Fig. 4). Quasi-phase-matching of any frequency conversion process is thus only limited by the ability to periodically pattern the nonlinear susceptibility.

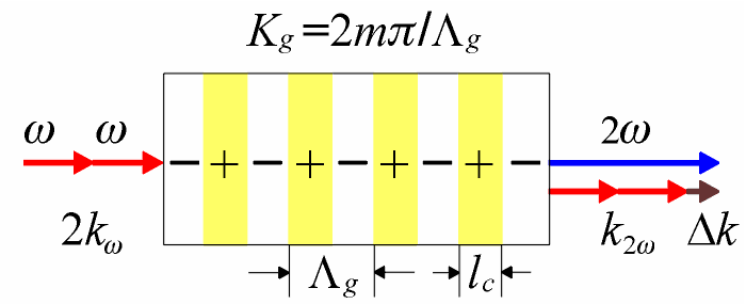

Fig. 4. Quasi-phase matching in the wave-vector space for collinear second-harmonic generation. The intrinsic wave-vector mismatch Δk of a particular wavelength can be canceled by proper design of grating period Λ_g.

In ferroelectric materials, the sign of the second order nonlinearity is related to the crystal orientation; alternation of the sign of the nonlinearity and hence QPM is achieved by periodic poling. Our method of periodic poling consists of applying a periodic electric field pattern on the ferroelectric wafer through a dielectric mask causing reversal of the domain orientation under the surface of the electrodes (Fig. 5). The so-formed periodic crystal orientation remains permanently after removal of the poling field. The dielectric mask is prepared lithographically which leads to high resolution as well as precise positioning. Such precise lithographic positioning of the gratings also allows full control of the phase of the generated light, making possible devices that employ interference effects, e.g., optically balanced mixers [16], as well as new devices suitable for pulse measurement [5-7,9].

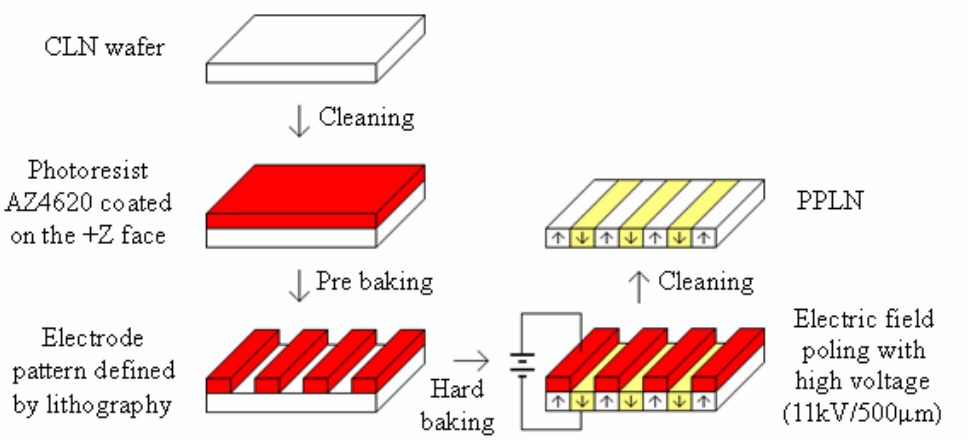

Fig. 5. A typical PPLN fabrication process (refer to Y.-C. Huang's group). CLN: congruent lithium niobate.

Waveguides

The efficiency of the frequency conversion process is significantly enhanced in waveguides where tight confinement of the interacting waves is maintained over long distances. The waveguide fabrication process is now briefly described (Fig. 6). After the periodic poling, an SiO_2 mask is sputtered on the +z or –z surface of the wafer, and channels are etched into the mask after lithographic definition in photoresist. The patterned channels are then proton exchanged (PE) in benzoic acid to form waveguides. PE gives a step-index profile (Δn_e=0.09 at 1550 nm), allowing for tight optical confinement (Fig. 7, first column). However, the propagation loss could be high (0.5-1 dB/cm), and there is a **dead layer** on the surface where $\chi^{(2)}$ nonlinearity is nearly erased [17]. A subsequent annealing step leads to the diffusion of protons deeper into the substrate, reducing the peak index change on the surface, smoothening the index profile (Fig. 7, second column), and partially recovering the surface $\chi^{(2)}$ [17]. This allows formation of diffused **channel (APE) waveguides** characterized by low loss (**0.2 dB/cm**) and high SHG conversion efficiency (up to **50 %/Wcm^2**, or 1250%/W for a 5-cm-long device) [4]. The modal peaks of fundamental and second-harmonic waves are nevertheless mismatched in the APE guides, for the highest index remains on the surface for either wavelength.

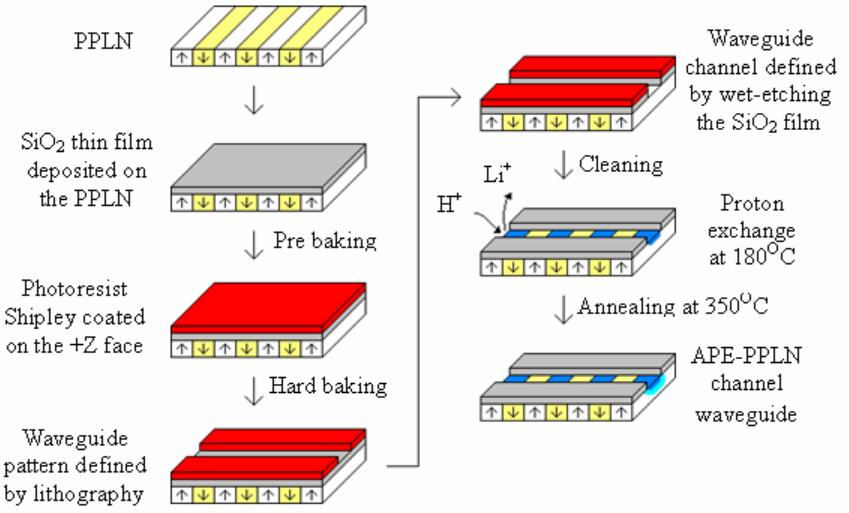

Fig. 6. A typical APE PPLN fabrication process (refer to Y.-C. Huang's group).

If an additional reverse proton exchange (RPE) step is added (e.g. immersion of the sample in a eutectic melt of $LiNO_3$:KNO_3:$NaNO_3$ for 10 hours at 328°C)**, where protons from the surface are replaced by lithium ions, a buried refractive index profile is realized allowing better modal overlap and even higher efficiency** (Fig. 7, third column) [4]. Our Stanford collaborators now routinely fabricate RPE waveguides with low loss (**<0.2 dB/cm**) and high efficiency (**150%/Wcm^2** or 6400%/W in 6-cm device). Because small variations in the mask width for the waveguide formation can cause non-uniform phase-matching along the guide and reduce the conversion efficiency, we use a non-critical waveguide design with vanishing first derivative of the phase-matching period with respect to waveguide width. These non-critical waveguide designs were employed in the high conversion efficiencies experiments cited above.

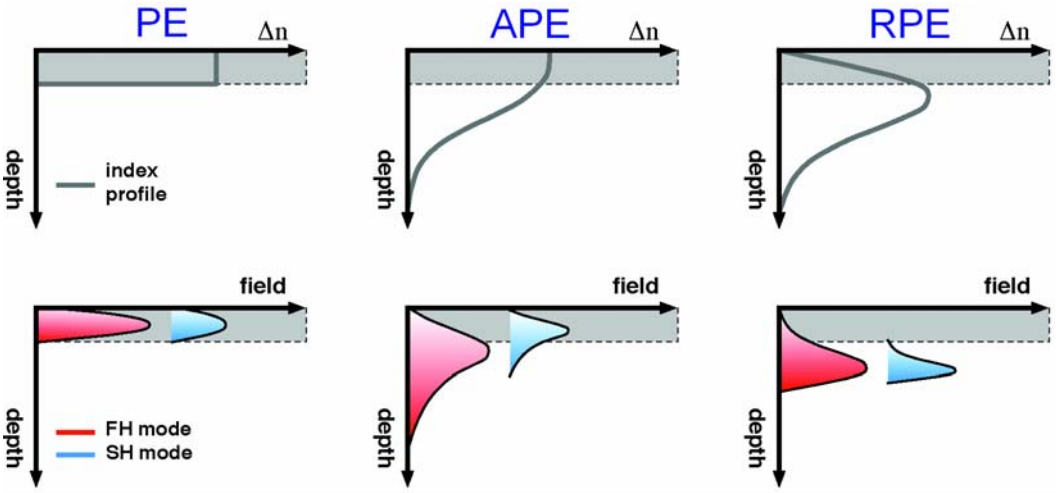

Fig. 7. Index profiles (first row) and mode profiles (second row) of proton exchange (PE), annealed proton exchange (APE), and reverse proton exchange (RPE) waveguides (courtesy of M. M. Fejer's group).

An important factor in waveguide device applications is efficient coupling into the device. A great advantage of our diffused APE and RPE waveguide technology is the ability to design tapers for input and output that provide very good mode matching between an optical fiber and the frequency conversion device. **The losses due to mode mismatch** to a standard single mode fiber are **~5%** for an RPE waveguide and 5-10% for an APE waveguide.

四、研究方法

The ambitious goal of this proposal is to break the world record of sensitivity of self-referenced complete femtosecond pulse measurement techniques by the marriage of modified interferometric field autocorrelation (MIFA) method [3] and the proprietary reverse proton exchange (RPE) PPLN waveguide technology [4] that have been established by our group at National Tsing Hua University and Prof. Martin M. Fejer's group at Stanford University, respectively. **The sensitivity improvement will not rely on expensive detection module** (like cooled intensified CCD camera used in delivering current world record [5,6,9]) **nor impractically long integration time** (say >20 minutes in [45]), **but theoretical novelty of MIFA method as well as the unparalleled conversion efficiency of RPE PPLN waveguide** (3 times better than APE counterpart).

I. Modified interferometric field autocorrelation (MIFA) method:

MIFA is a new method proposed and experimentally demonstrated by our group to analytically (non-iteratively) reconstruct spectral phase profile by measuring double one-dimensional interferometric autocorrelation traces using thick nonlinear crystals [3].

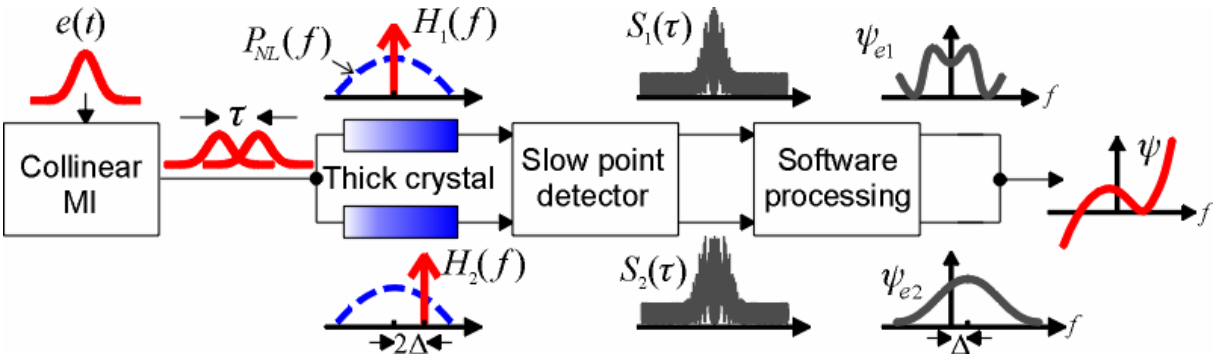

Fig. 8. Schematic diagram of MIFA measurement. MI: Michelson interferometer.

Fig. 8 illustrates the schematic diagram of MIFA measurement. The scalar e-field of the pulse is represented by: $e(t) = \mathrm{Re}\left\{a(t)e^{j2\pi f_0 t}\right\}$, where Re[ ] denotes real part, $a(t)$ is the complex temporal envelope, and f_0 represents the carrier frequency, respectively. A collinear Michelson interferometer produces a pulse pair $e_\omega(t) = e(t) + e(t-\tau)$ (τ is the variable delay), corresponding to a nonlinear polarization spectrum $P_{NL}(f) = F\left\{e_\omega^2(t)\right\}$ centered at $2f_0$ ($F\{\ldots\}$ denotes Fourier transform). By using a thick nonlinear crystal with narrow phase-matching spectrum $H_1(f)$ centered at $2f_0$, the generated second-harmonic spectrum and average power are proportional to $P_{NL}(f)\cdot H_1(f) \propto P_{NL}(2f_0)$ and:

$$S_1(\tau) \propto 1 + 2\left|G_1'(\tau)\right|^2 + 4\,\mathrm{Re}[G_1'(\tau)]\cos(2\pi f_0\tau) + \cos(4\pi f_0\tau)\,, \tag{4}$$

respectively, where the modified field autocorrelation function is defined as [3]:

$$G_1'(\tau) \equiv \left\langle a(t)a(t-\tau)\right\rangle \Big/ \left\langle a^2(t)\right\rangle \tag{5}$$

The Fourier transform of eq. (4), denoted by $\tilde{S}_1(\kappa)$, consists of five spectral components centered at delay-frequencies of $\kappa = 0$, $\pm f_0$, and $\pm 2f_0$, respectively. By extracting the components centered at $\kappa = 0$ and $\kappa = f_0$, we can get the modulus and real part of $G_1'(\tau)$ ($\left|G_1'(\tau)\right|$ and $\mathrm{Re}[G_1'(\tau)]$), respectively. This enables the determination of the complex function $G_1'(\tau)$ for the phase of $G_1'(\tau)$ can be evaluated by:

$$\angle G_1'(\tau) = \cos^{-1}\{\mathrm{Re}[G_1'(\tau)]/|G_1'(\tau)|\}\,.$$

The Fourier transform of eq. (5) becomes:

$$\tilde{G}_1'(f) \propto A(f)A(-f) = \left|A(f)A(-f)\right|\exp\{j[\psi(f) + \psi(-f)]\} \tag{6}$$

where $A(f) = F\{a(t)\} = |A(f)|e^{j\psi(f)}$ stands for the spectral envelope of the pulse. The phase of

eq. (6), $\psi(f)+\psi(-f)$, is an even function of baseband frequency f, providing all spectral phase components symmetric with respect to carrier frequency f_0:

$$\psi_{e1}(f) \equiv \frac{\psi(f)+\psi(-f)}{2} = \frac{\angle \tilde{G}_1'(f)}{2} \tag{7}$$

Complete (second order and higher) spectral phase retrieval can be accomplished if we measure a second MIFA trace $S_2(\tau)$ by using a narrow PM spectrum $H_2(f)$ centered at $2(f_0-\Delta)$ (can be achieved by tuning the PM angle of a birefringent crystal or changing the temperature of a quasi-phase matched grating). The aforementioned procedures give rise to an even function of variable $f-\Delta$ (neither even nor odd in terms of variable f), providing all spectral phase components symmetric with respect to carrier frequency $f_0-\Delta$:

$$\psi_{e2}(f) \equiv \frac{\psi(f)+\psi(-f-2\Delta)}{2} \tag{8}$$

Combining equations (7) and (8), we can derive a recursive relation to reconstruct the spectral phase $\psi(f)$ of the pulse (with a resolution of 2Δ):

$$\psi(f-2\Delta)-\psi(f) = 2[\psi_{e2}(f-2\Delta)-\psi_{e1}(f)] \tag{9}$$

Equations (7-9) show that the capability of spectrally selective "even" phase retrieval of MIFA method allows for analytic phase reconstruction by using two one-dimensional correlation traces.

II. Why MIFA+PPLN can be more sensitive than FROG+A-PPLN:

The current world record of sensitivity of self-referenced complete femtosecond pulse measurement (2.7×10^{-6} mW^2) was achieved by employing 6-cm-long annealed proton exchange (APE) aperiodically poled lithium niobate (A-PPLN) waveguide [9]. This result is primarily enabled by: (1) Tight optical confinement due to the waveguide structure. (2) Broad phase-matching bandwidth due to linearly chirped QPM period. In this proposal, we intend to lever two unique advantages of MIFA method to surpass the previous record.

1) **MIFA only takes one-dimensional data sets**. As shown in Fig. 8, **MIFA** measures the second-harmonic power "value" for each delay τ (one-dimensional trace). This means that MIFA does not spatially disperse the output beam, and **all the second-harmonic power can be measured by one point detector**. In contrast, **FROG** (Fig. 2) needs to disperse the beam to take the second-harmonic power "spectrum" for each delay τ (two-dimensional trace), and **each pixel of the detector array can only measure a small fraction of the second-harmonic power**. Using a scanning monochrometer in FROG can only eliminate the requirement of detector array, while the detection efficiency remains inferior to those of 1-D techniques. As a result, the reported sensitivity record of intensity autocorrelation (3.2×10^{-7} mW^2) [7] remains 8 times better than that of FROG, though they used the same APE PPLN waveguide.

2) **MIFA can make use of "available nonlinearity" more efficiently**. Consider second-harmonic generation of a short pulse with complex envelope $a(t)$. The averaged second-harmonic power is proportional to the overlap integral:

$$\langle P_{2\omega} \rangle \propto \int_{-\infty}^{\infty} |P_{NL}(f)|^2 \times |H(f)|^2 df \,, \tag{10}$$

where $P_{NL}(f)=F\{a^2(t)\}$ and $H(f)$ represent the nonlinear polarization spectrum of the input pulse and the phase-matching spectrum provided by the nonlinear crystal, respectively. The **"available nonlinearity", defined as the phase-matching spectral area**:

$$\eta_{NL}=\int_{-\infty}^{\infty}|H(f)|^2 df\ , \tag{11}$$

can be used as a measure about the "potential" of the nonlinear crystal to produce second-harmonic yield. Under the condition of non-depleted pump, a uniform nonlinear crystal of length L (including PPLN) provides:

$$H(f)\propto L\cdot\mathrm{sinc}(\pi\eta Lf),\quad \eta=v_g^{-1}(2f_0)-v_g^{-1}(f_0) \tag{12}$$

where v_g denotes group velocity, and f_0 is the fundamental carrier frequency. Chirping the QPM period (A-PPLN) may broaden the width of $H(f)$ without changing the "available nonlinearity" η_{NL} [7].

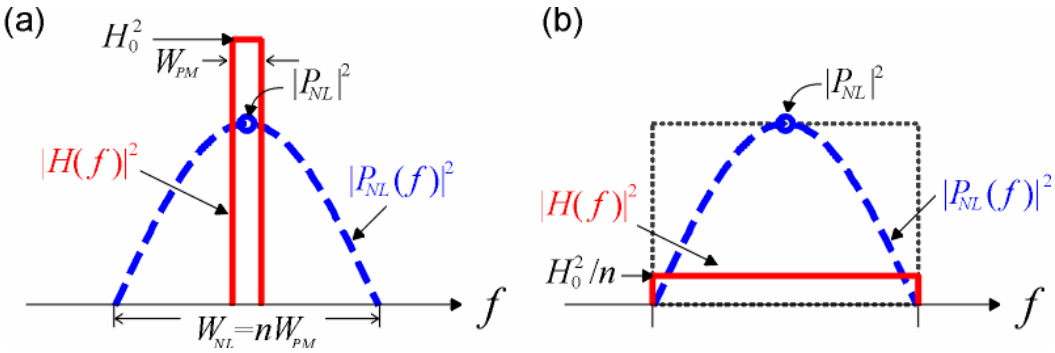

Fig. 9. Spectral representations of pulsed second-harmonic generation using (a) thick PPLN in MIFA, (b) thick A-PPLN in intensity autocorrelation.

For simplicity, we approximate $|H(f)|^2$ due to a PPLN of length L by a rectangular function of width W_{PM} ($\propto L^{-1}$) and height H_0^2 ($\propto L^2$), while $|P_{NL}(f)|^2$ has a width $W_{NL}=nW_{PM}$ (n>>1) and a peak value $|P_{NL}|^2$ (Fig. 9a). Since the phase-matching bandwidth W_{PM} is much narrower than the nonlinear polarization bandwidth W_{NL}, this configuration can be used in MIFA measurement. By eq. (10), the corresponding second-harmonic yield is:

$$\langle P_{2\omega}\rangle_{MIFA}\propto|P_{NL}|^2H_0^2W_{PM}=\frac{|P_{NL}|^2H_0^2W_{NL}}{n}\ . \tag{13}$$

On the other hand, to conduct intensity autocorrelation by using A-PPLN of the same length L, the QPM period has to be properly chirped such that $|H(f)|^2$ becomes a rectangular function of width nW_{PM}. In this case, the height of $|H(f)|^2$ is reduced to H_0^2/n such that the area of $|H(f)|^2$ remains (Fig. 9b). By eq. (10), the corresponding second-harmonic yield is:

$$\langle P_{2\omega}\rangle_{IA}\propto\int_{-\infty}^{\infty}|P_{NL}(f)|^2\frac{H_0^2}{n}df<\int_{W_{NL}}|P_{NL}|^2\frac{H_0^2}{n}df=\langle P_{2\omega}\rangle_{MIFA} \tag{14}$$

Eq's (13), (14) show that **the second-harmonic yield improvement factor *F*** is:

$$F = \frac{\langle P_{2\omega} \rangle_{MIFA}}{\langle P_{2\omega} \rangle_{IA}} = \frac{\int_{W_{NL}} |P_{NL}|^2 df}{\int_{W_{NL}} |P_{NL}(f)|^2 df} \geq 1, \tag{15}$$

which is the ratio of area $|P_{NL}|^2 W_{NL}$ of a rectangle (dotted in Fig. 9b) to the area of $|P_{NL}(f)|^2$. Eq. (15) means that the improvement factor depends on the shape of $|P_{NL}(f)|^2$ (thus the complex spectrum of the input pulse).

Combining the two effects discussed above, together with **the second-harmonic yield improvement (by a factor of 3) provided by the RPE waveguides** over the APE counterparts, **we expect to improve on the world record by a factor of 8×2.5×3=60 at best**.

五、結果與討論

We have successfully achieved what we promised to carry out. Our experiment achieved a sensitivity of 1.1×10^{-7} mW^2, improving on the previous record by a factor of 20. Beyond that, we have extended the scheme to measure the power spectrum of the input pulse. As a result, MIFA is able to retrieve the complex spectrum (as FROG, and better than SPIDER) with unprecedented measurement sensitivity. **The key results have been published in Optics Letters and selected by Virtual Journal of Ultrafast Science** [19].

1) Theoretical achievement:

The complex spectrum of the modified field autocorrelation function, shown in eq. (6), can be rewritten as:

$$\tilde{G}_1'(f) \propto P_{e1}(f) \exp[j2\psi_{e1}(f)], \tag{16}$$

where

$$P_{e1}(f) = |A(f)A(-f)|$$

represents the even spectral intensity. Similarly, the second MIFA trace contributes to:

$$\psi_{e2}(f) \equiv [\psi(f) + \psi(-f + 2\Delta)]/2$$

as shown in eq. (8), as well as:

$$P_{e2}(f) = |A(f)A(-f - 2\Delta)|,$$

representing the even spectral intensity with respect to $2(f_0 - \Delta)$. A new recursive relation:

$$\left|\frac{A(f-2\Delta)}{A(f)}\right|^2 = \left[\alpha \frac{P_{e2}(f-2\Delta)}{P_{e1}(f)}\right]^2 \tag{17}$$

is used to reconstruct the power spectrum. When $P_{e1}(f)$ and $P_{e2}(f)$ are normalized to:

$$P_{e1}(0) = P_{e2}(-\Delta) = 1,$$

the constant α in eq. (17) becomes:

$$\alpha = \left| \frac{A(0)}{A(-\Delta)} \right|^2 \tag{18}$$

Since the α constant is typically obtained by an optical spectrum analyzer, the usefulness of eq. (17) lies mainly in the inherent consistency check of the experimental data traces.

2) Experiments:

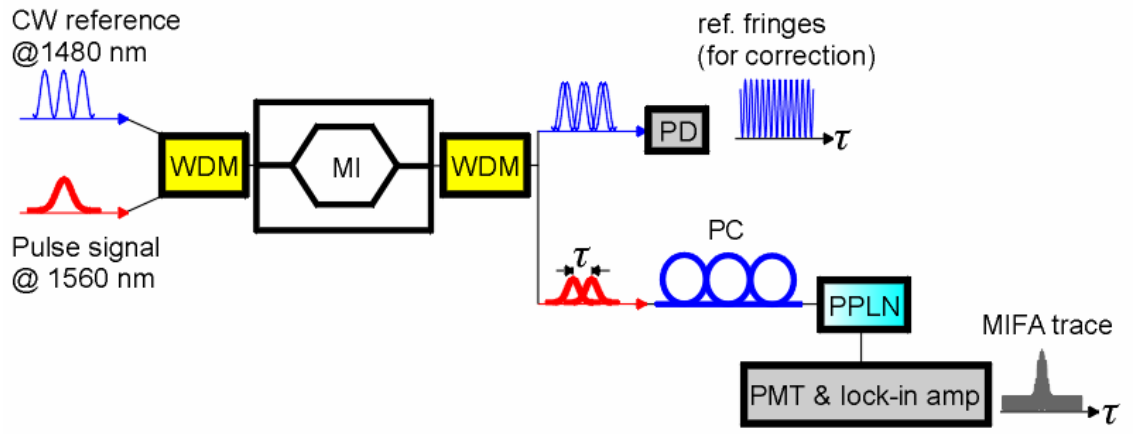

Fig. 10. Experimental setup of high sensitivity MIFA measurement. WDM: Wavelength division multiplexer. MI: Michelson interferometer. PC#: polarization controller. PD: InGaAs photodetectors.

Fig. 10 shows the fiber-based experimental setup for our ultra-sensitive MIFA measurement. The signal pulse at 1560 nm comes from a passively mode-locked Er-doped fiber laser, and is combined with the CW reference at 1480 nm using a wavelength division multiplexer. They are sent into a collinear Michelson interferometer, where an electrically controlled delay line (VariDelay II, General photonics) is used to scan the optical delay at a speed of 1 ps per second. The interfered CW reference goes to an InGaAs photodetector by way of another wavelength division multiplexer, producing a trace used for fringe correction. The signal pulse pair are coupled into a fiber-pigtailed PPLN waveguide with a 49-mm-long QPM grating for SHG. The PM tuning curve of the PPLN waveguide has a sinc^2-shape with an FWHM of ~0.24 nm (phase-matching bandwidth ~50 GHz, much smaller than the pulse bandwidth of 10 nm or 1.25 THz), and the peak wavelengths are set at 1559.86 nm and 1560.34 nm (PPLN temperature at 46°C and 50°C) when acquiring the two MIFA traces, respectively. The average second-harmonic power at each delay is detected by a PMT (R636-10, Hamamatsu) and lock-in amplifier. The lock-in time constant is set at 0.64 ms (limited by the scanning speed of the delay line and the required delay resolution), corresponding to a delay resolution of 0.64 fs (better than the Nyquist criterion of $0.25 f_0$ =1.3 fs). It only takes 10 seconds to acquire one MIFA trace with a 10-ps delay window.

Fig. 11a illustrates the retrieved spectral phase profiles of a nearly bandwidth-limited pulse at average powers (coupled into the waveguide) of 1.5 nW (dashed-dotted) and 2.6 μW (dotted), respectively. In the presence of a 32 dB input power difference (64 dB difference in SHG powers),

the retrieved spectral phase profiles agree well with each other. Fig. 11b shows the evaluated temporal intensity of the pulse based on the retrieved spectral phase and the power spectrum measured by the OSA. The pulse width (FWHM) is 374 fs. The pulse shape exhibits some asymmetric oscillating tails, which is a signature of the residual cubic spectral phase. The 1.5 nW average power is equivalent to 75 μW peak power, 28 aJ pulse energy, corresponding to an unprecedented sensitivity of 1.1×10^{-7} mW^2.

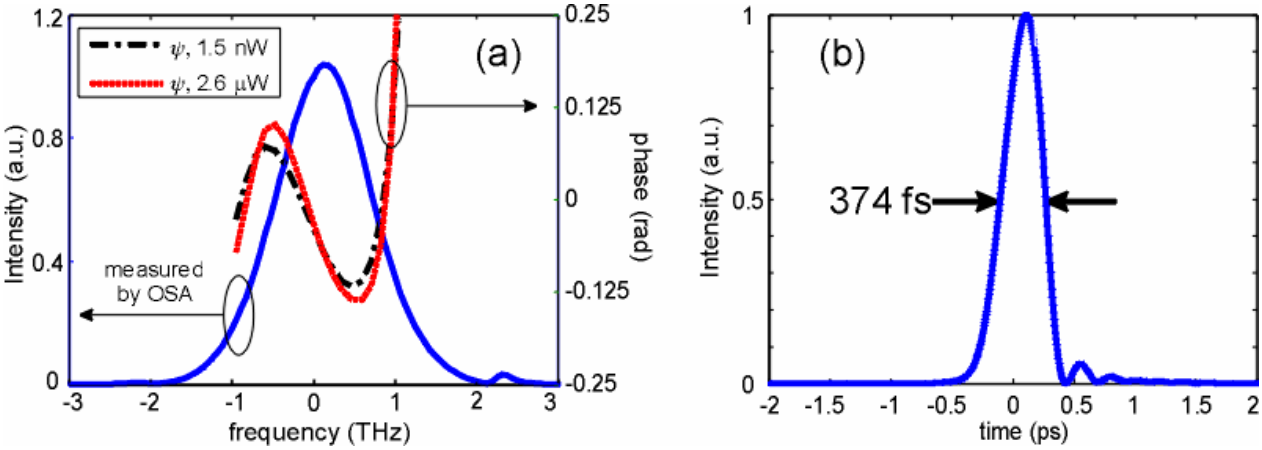

Fig. 11. (a) Retrieved spectral phase profiles for input average powers of 1.5 nW (dashed-dotted) and of 2.6 μW (dotted). (b) Retrieved temporal intensity profile.

We have successfully achieved the original goal of the proposal. The measurement sensitivity is improved by a factor of 20, close to the most optimistic value of 60 predicted in the proposal. The difference can be attributed to two major factors. (1) The PPLN waveguide used in our experiment is shorter than that used in [7] (49 mm vs. 59 mm), resulting in lower SHG conversion efficiency. (2) The lock-in time constant in our experiment is relatively short compared with that in [9] (0.64 ms vs. 800 ms). The short time constant leads to larger noise background, degrading the measurement sensitivity. We could not use longer time constant for the scanning speed of our variable delay line has to be faster than 1 ps per second, otherwise, the mechanical vibration would become too strong to get clear interferometric fringes. By solving these two problems, the sensitivity improvement factor should be able to approach 60.

The all-fiber-based setup is nearly alignment-free, can acquire data traces in 20 seconds, only needs cost-effective point detector, and can deliver complex field without iterative data inversion. These facts prove the usefulness of MIFA scheme in practical applications. We are also working on demonstrating the advantages of MIFA in measuring extremely short (<10 fs) pulses.

Our work also shows that MIFA can be applied in analyzing “interferometric spectrogram” [20], a data set also known as interferometric FROG (iFROG) trace (Fig. 12a). Previously, interferometric spectrogram was processed by either low-pass filtering to get standard FROG trace and thus complex field [21] or MEFISTO method to get the spectral phase profile non-iteratively [22]. We experimentally showed that the same interferometric spectrogram data can be processed by FROG, MEFISTO, and MIFA to get mutually consistent solutions (Fig. 12cd). Additionally, an interferometric spectrogram is sufficient to give rise to multiple solutions

of spectral phase profile by using MIFA processing, and the weighted average of these solutions gives a more robust solution (close to that obtained by FROG) against the measurement noise. This work has been **published in Optics Express in 2010** [20].

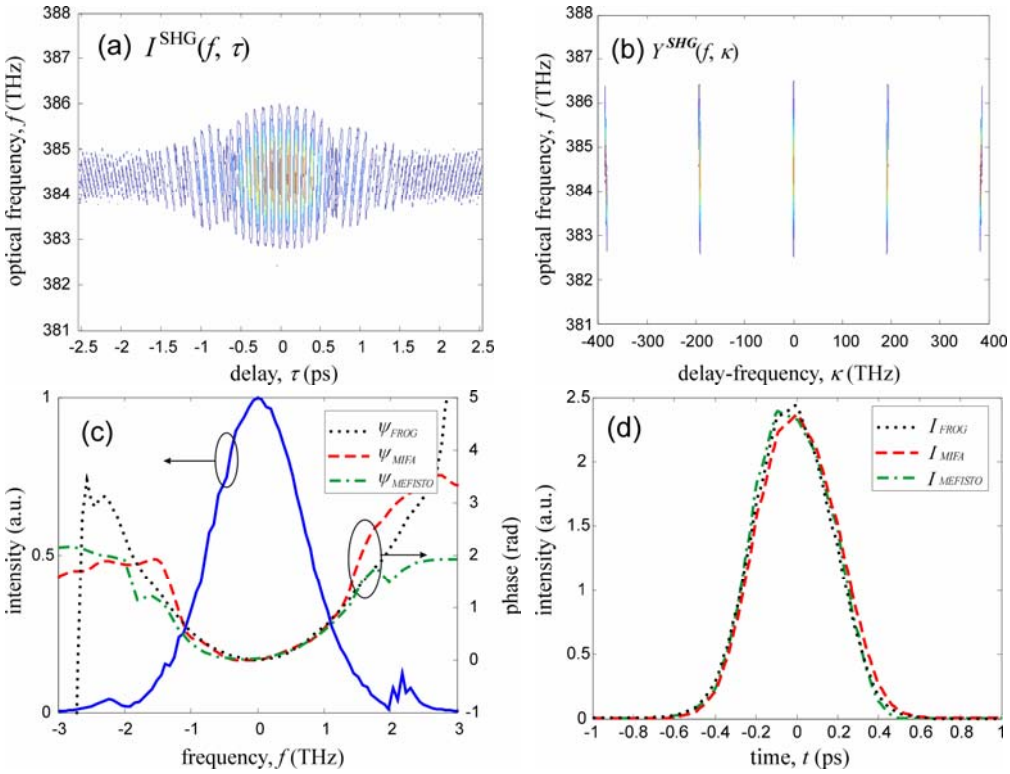

Fig. 12. (a) Experimentally measured interferometric spectrogram, and (b) its Fourier transform with respect to delay. For clarity, Fig. 12b is manipulated to highlight the components around $\kappa = \pm f_0$. (c) Spectral phase profiles, and (d) temporal intensity profiles measured by FROG (dotted), MIFA (dashed), and MEFISTO (dash-dot), respectively. The solid line in Fig. 12c represents the fundamental power spectrum measured by OSA.

參考文獻：

1. N. Dudovich, D. Oron, Y. Silberberg, “Single-pulse coherently controlled nonlinear Raman spectroscopy and microscopy,” *Nature,* **418**, 512-514 (2002).
2. M. Yamashita, K. Yamane, R. Morita, “Quasi-automatic phase-control technique for chirp compensation of pulses with over-one-octave bandwidth− generation of few- to mono-cycle optical pulses,” *IEEE J. Sel. Topics Quantum Electron.,* **12**, 213-222 (2006).
3. Shang-Da Yang, Chen-Shao Hsu, Shih-Lun Lin, Houxun Miao, Chen-Bin Huang, and Andrew M. Weiner, “Direct spectral phase retrieval of ultrashort pulses by double modified one-dimensional autocorrelation traces,” *Optics Express*, **16**(25), 20617-20625 (2008).
4. K. R. Parameswaran, R. K. Route, J. R. Kurz, R. V. Roussev, M. M. Fejer, “Highly efficient second-harmonic generation in buried waveguides formed by annealed and reverse proton exchange in periodically poled lithium niobate,” *Opt. Lett.,* **27**, 179-181 (2002).
5. H. Miao, S. -D. Yang, C. Langrock, R. V. Roussev, M. M. Fejer, A. M. Weiner, “Ultralow-power second-harmonic generation frequency-resolved optical gating using aperiodically poled lithium niobate waveguides,” *J. Opt. Soc. Am. B,* **25**, A41-A53 (2008).
6. S. -D. Yang, H. Miao, Z. Jiang, A. M. Weiner, K. R. Parameswaran, M. M. Fejer, “Ultrasensitive nonlinear measurements of femtosecond pulses in the telecommunications band by aperiodically poled $LiNbO_3$ waveguides,” *Appl. Optics*, **46**, 6759-6769 (2007).
7. Shang-Da Yang, Andrew M. Weiner, Krishnan R. Parameswaran, and Martin M. Fejer, “400-photon-per-pulse ultrashort pulse autocorrelation measurement with aperiodically poled lithium niobate waveguides at 1.55 μm,” *Opt. Lett.*, **29**(17), 2070-2072, (2004).
8. R. Trebino, *Frequency-resolved optical gating: the measurement of ultrashort laser pulses* (Kluwer Academic Publishers, 2000).
9. Shang-Da Yang, Andrew M. Weiner, Krishnan R. Parameswaran, and Martin M. Fejer, “Ultra-sensitive second-harmonic generation frequency-resolved optical gating by aperiodically poled $LiNbO_3$ waveguides at 1.5 μm,” *Opt. Lett.*, **30**(16), 2164-2166, (2005).
10. C. Iaconis, I. A. Walmsley, “Spectral phase interferometry for direct electric-field reconstruction of ultrashort optical pulses,” *Opt. Lett.,* **23**, 792-794 (1998).
11. C. Dorrer, P. Londero, I.A. Walmsley, “Homodyne detection in spectral phase interferometry for direct electric-field reconstruction”, *Opt. Lett.,* **26**(19), 1510-1512, (2001).
12. J. Bromage, C. Dorrer, I.A. Begishev, N.G. Usechak, J.D. Zuegel, “Highly sensitive, single-shot characterization for pulse widths from 0.4 to 85 ps using electro-optic shearing interferometry”, *Opt. Lett.,* **31**(23), 3523-3525, (2006).
13. A. S. Radunsky, E. M. Kosik, Williams, I. A. Walmsley, “Simplified spectral phase interferometry for direct electric-field reconstruction by using a thick nonlinear crystal”, *Opt. Lett.,* **31**(7), 1008-1010, (2006).
14. J. R. Kurz, J. Huang, X. Xie, T. Saida, M. M. Fejer, “Mode multiplexing in optical frequency mixers,” *Opt. Lett.,* **29**(6), 551-553 (2004).

15. C. Langrock, M. M. Fejer, “Background-free collinear autocorrelation and frequency-resolved optical gating using mode multiplexing and demultiplexing in aperiodically poled lithium niobate waveguides,” Opt. Lett., **32**(16), 2306-2308, (2007).
16. J. R. Kurz, K. R. Parameswaran, R. V. Roussev, M. M. Fejer, "Optical-Frequency Balanced Mixer," Opt. Lett., **26**, 1283-1285, (2001).
17. M. L. Bortz, L. A. Eyres, M. M. Fejer, "Depth profiling of the d_{33} nonlinear coefficient in annealed proton exchanged $LiNbO_3$ waveguides," Appl. Phys. Lett., **62**, 2012-2014, (1993).
18. J.-Y Zhang, A. P. Shreenath, M. Kimmel, E. Zeek, R. Trebino, “Measurement of intensity and phase of attojoule femtosecond light pulses using optical-parametric- amplification cross-correlation frequency-resolved optical gating”, Opt. Express, **11**(6), 601-609, (2003).
19. Shang-Da Yang, Chen-Shao Hsu, Shih-Lun Lin, You-Sheng Lin, Carsten Langrock, and M. M. Fejer, “Ultrasensitive direct-field retrieval of femtosecond pulses by modified interferometric field autocorrelation,” *Opt. Lett.*, **34**(20), 3065-3067, (2009).
20. Li-Fan Yang, Shih-Lun Lin, and Shang-Da Yang, "Ultrashort pulse measurements by interferometric spectrogram," *Optics Express*, **18**(7), 6877-6884, (2010).
21. I. Amat-Roldan, I. G. Cormack, P. Loza-Alvarez, E. J. Gualda, D. Artigas, “Ultrashort pulse characterization with SHG collinear-FROG”, *Opt. Express,* **12**(6), 1169-1178, (2004).
22. I. Amat-Roldan, I. G. Cormack, P. Loza-Alvarez, “Measurement of electric field by interferometric spectral trace observation”, *Opt. Lett.,* **30**(9), 1063-1065, (2005).

附件二

國科會補助專題研究計畫成果報告自評表

請就研究內容與原計畫相符程度、達成預期目標情況、研究成果之學術或應用價值（簡要敘述成果所代表之意義、價值、影響或進一步發展之可能性）、是否適合在學術期刊發表或申請專利、主要發現或其他有關價值等，作一綜合評估。

1. 請就研究內容與原計畫相符程度、達成預期目標情況作一綜合評估

☑ 達成目標

☐ 未達成目標（請說明，以 100 字為限）

☐ 實驗失敗

☐ 因故實驗中斷

☐ 其他原因

說明：

2. 研究成果在學術期刊發表或申請專利等情形：

論文：☑已發表 ☐未發表之文稿 ☐撰寫中 ☐無

專利：☐已獲得 ☐申請中 ☐無

技轉：☐已技轉 ☐洽談中 ☐無

其他：（以 100 字為限）

3. 請依學術成就、技術創新、社會影響等方面，評估研究成果之學術或應用價值（簡要敘述成果所代表之意義、價值、影響或進一步發展之可能性）（以 500 字為限）

Our work has experimentally verified that MIFA method is the most sensitive pulse measurement technique, capable of retrieving amplitude and phase of a pulse train with average pulse energy of ~200 photons. The simple, all-fiber based, cost-effective configuration makes MIFA a promising technique as a daily tool in ultrafast laser diagnostics. The future works lie in: (1) Measurement even shorter (<10 fs) pulses. (2) Measuring even weaker pulses by increasing the data integration time. (3) Measuring vector fields (amplitude, phase, polarization).

附件三

國科會補助計畫衍生研發成果推廣資料表

日期：99 年 10 月 30 日

<table>
<tr><td>國科會補助計畫</td><td colspan="3">計畫名稱：使用反質子交換週期性區域反轉鈮酸鋰波導及修正場自相關技術突破飛秒脈衝量測靈敏度極限
計畫主持人：楊尚達
計畫編號：NSC 98-2221-E-007-031　　領域：EE</td></tr>
<tr><td rowspan="2">研發成果名稱</td><td colspan="3">（中文）以修正場自相關技術量測超微弱飛秒光脈衝</td></tr>
<tr><td colspan="3">（英文）Ultrasensitive femtosecond pulse measurement by modified interferometric field autocorrelation technique</td></tr>
<tr><td>成果歸屬機構</td><td>國科會</td><td>發明人
（創作人）</td><td>楊尚達</td></tr>
<tr><td rowspan="2">技術說明</td><td colspan="3">（中文）傳統之飛秒脈衝完全量測有兩大限制：(一)因非線性轉換效率不足，需要輸入強大之脈衝能量。(二)量測取得之大量原始數據需經緩慢之疊代計算方能擷取脈衝資訊。本技術應用週期性區域反轉之鈮酸鋰光波導及簡單之麥克生干涉儀可直接(無疊代)解析出僅 28 aJ 的超短脈衝光場。</td></tr>
<tr><td colspan="3">（英文）Traditional femtosecond pulse measurements are limited by: (1) high power requirement for insufficient conversion efficiency; (2) recorded data needs time-consuming iterative retrieval to reconstruct the pulse information. This technique applies for periodically poled lithium niobate waveguides and Michelson interferometer, which can directly retrieve the amplitude and phase of a 28-aJ, 374-fs pulse train without iterative data inversion.</td></tr>
<tr><td>產業別</td><td colspan="3">雷射光電科技</td></tr>
<tr><td>技術/產品應用範圍</td><td colspan="3">1. 光訊號檢測儀器
2. 光學示波器
3. 任意光訊號產生器</td></tr>
<tr><td>技術移轉可行性及預期效益</td><td colspan="3">目前超短脈衝量測儀器的商用產品選項不多，價格昂貴(約 2 萬美元)。本技術成本低廉、功能強大，可望有助於光訊號檢測儀器之開發。</td></tr>
</table>

註：**本項研發成果若尚未申請專利，請勿揭露可申請專利之主要內容。**

國科會補助計畫衍生研發成果推廣資料表

日期:2010/11/05

國科會補助計畫	計畫名稱: 使用反質子交換週期性區域反轉鈮酸鋰波導及修正場自相關技術突破飛秒脈衝量測靈敏度極限		
	計畫主持人: 楊尚達		
	計畫編號: 98-2221-E-007-031- 學門領域: 量子電子學與雷射科技		
研發成果名稱	(中文) 以修正場自相關技術量測超微弱飛秒光脈衝		
	(英文) Ultrasensitive femtosecond pulse measurement by modified interferometric field autocorrelation technique		
成果歸屬機構	國立清華大學	發明人(創作人)	楊尚達
技術說明	(中文) 傳統之飛秒脈衝完全量測有兩大限制：(一)因非線性轉換效率不足，需要輸入強大之脈衝能量。(二)量測取得之大量原始數據需經緩慢之疊代計算方能擷取脈衝資訊。本技術應用週期性區域反轉之鈮酸鋰(periodically poled lithium niobate)光波導及簡單之麥克生干涉儀，一方面大幅提高非線性轉換效率，一方面減少原始數據資料量並以非疊代演算法直接解析出脈衝的振幅及相位。實驗上證實可以量出平均能量僅28 attojoule的超短脈衝序列。		
	(英文) Traditional femtosecond pulse measurements are limited by: (1) high power requirement for insufficient conversion efficiency; (2) recorded data needs time-consuming iterative retrieval to reconstruct the pulse information. This technique applies for periodically poled lithium niobate waveguides and Michelson interferometer, which can directly retrieve the amplitude and phase of a 28-aJ, 374-fs pulse train without iterative data inversion.		
產業別	檢測維護業；光學及精密器械製造業		
技術/產品應用範圍	光訊號檢測儀器，光學示波器，任意光訊號產生器		
技術移轉可行性及預期效益	目前超短脈衝量測儀器的商用產品選項不多，價格昂貴(約2萬美元)。本技術成本低廉、功能強大，可望有助於光訊號檢測儀器之開發。		

註：本項研發成果若尚未申請專利，請勿揭露可申請專利之主要內容。

98 年度專題研究計畫研究成果彙整表

計畫主持人：楊尚達	計畫編號：98-2221-E-007-031-
計畫名稱：使用反質子交換週期性區域反轉鈮酸鋰波導及修正場自相關技術突破飛秒脈衝量測靈敏度極限	

成果項目			量化			單位	備註（質化說明：如數個計畫共同成果、成果列為該期刊之封面故事...等）
			實際已達成數（被接受或已發表）	預期總達成數(含實際已達成數)	本計畫實際貢獻百分比		
國內	論文著作	期刊論文	1	1	100%	篇	物理雙月刊
		研究報告/技術報告	0	0	100%		
		研討會論文	1	1	100%		OPT 2009 口頭報告
		專書	0	0	100%		
	專利	申請中件數	0	0	100%	件	
		已獲得件數	0	0	100%		
	技術移轉	件數	0	0	100%	件	
		權利金	0	0	100%	千元	
	參與計畫人力（本國籍）	碩士生	2	2	100%	人次	
		博士生	1	1	100%		
		博士後研究員	0	0	100%		
		專任助理	0	0	100%		
國外	論文著作	期刊論文	2	2	100%	篇	發表於 Optics Letters, Optics Express 各 1 篇. 其中發表於 OL 者入選 Virtual Journal of Ultrafast Science.
		研究報告/技術報告	0	0	100%		
		研討會論文	2	2	100%		
		專書	0	0	100%	章/本	
	專利	申請中件數	0	0	100%	件	
		已獲得件數	0	0	100%		
	技術移轉	件數	0	0	100%	件	
		權利金	0	0	100%	千元	
	參與計畫人力（外國籍）	碩士生	0	0	100%	人次	
		博士生	0	0	100%		
		博士後研究員	1	1	100%		
		專任助理	0	0	100%		

其他成果 (無法以量化表達之成果如辦理學術活動、獲得獎項、重要國際合作、研究成果國際影響力及其他協助產業技術發展之具體效益事項等，請以文字敘述填列。)	獲 Coherent-Superbin Best Paper Award in the 6th Asian Conference on Ultrafast Phenomena 2010. 與 Ginzton Lab of Stanford University 成功合作。 打破飛秒脈衝量測靈敏度世界記錄，性能提升 20 倍。

	成果項目	量化	名稱或內容性質簡述
科教處計畫加填項目	測驗工具(含質性與量性)	0	
	課程/模組	0	
	電腦及網路系統或工具	0	
	教材	0	
	舉辦之活動/競賽	0	
	研討會/工作坊	0	
	電子報、網站	0	
	計畫成果推廣之參與（閱聽）人數	0	

國科會補助專題研究計畫成果報告自評表

請就研究內容與原計畫相符程度、達成預期目標情況、研究成果之學術或應用價值（簡要敘述成果所代表之意義、價值、影響或進一步發展之可能性）、是否適合在學術期刊發表或申請專利、主要發現或其他有關價值等，作一綜合評估。

1. 請就研究內容與原計畫相符程度、達成預期目標情況作一綜合評估

■達成目標

□未達成目標（請說明，以 100 字為限）

□實驗失敗

□因故實驗中斷

□其他原因

說明：

2. 研究成果在學術期刊發表或申請專利等情形：

論文：■已發表 □未發表之文稿 □撰寫中 □無

專利：□已獲得 □申請中 ■無

技轉：□已技轉 □洽談中 ■無

其他：(以 100 字為限)

3. 請依學術成就、技術創新、社會影響等方面，評估研究成果之學術或應用價值（簡要敘述成果所代表之意義、價值、影響或進一步發展之可能性）(以 500 字為限)

Our work has verified that MIFA is the most sensitive pulse measurement technique, capable of retrieving amplitude and phase of a pulse train with average pulse energy of ~200 photons. The simple, all-fiber based, cost-effective configuration makes MIFA a promising technique as a daily tool in ultrafast laser diagnostics. The future works include: (1) Measurement even shorter (<10 fs) pulses. (2) Measuring even weaker pulses by increasing the data integration time. (3) Measuring vector fields (amplitude, phase, polarization).